2014 IEEE 17th International Conference on
Intelligent Transportation Systems (ITSC)
October 8-11, 2014. Qingdao, China

Collision avoidance at intersections: A probabilistic threat-assessment and decision-making system for safety interventions *

Gabriel R. de Campos [1], Adam H. Runarsson [2], Fredrik Granum [2], Paolo Falcone [1], Klas Alenljung [3]

***Abstract*— Road intersections are among the most complex and accident-prone elements of modern traffic networks. Thus, new safety systems have to cope with highly complex traffic scenarios where the behavior of the different road users is difficult to predict. Sensing the surrounding environment and assessing possible threats therefore remain challenging problems. This paper provides a novel, efficient active-safety system for frontal collisions detection and prevention/mitigation. More precisely, we provide: (i) a probabilistic motion prediction algorithm based on an unscented Kalman filter; (ii) a probabilistic threat assessment method based on vectors defined by reference points on the vehicles' structure; (iii) a reachability-based decision-making protocol enabling an emergency intervention. Simulation results, based on realistic data obtained specifically for this scenario, are also presented showing the efficiency and the potential of the proposed solution.**

I. INTRODUCTION

Traffic control at intersections is a particularly challenging problem for new intelligent transportation systems. Indeed, road intersections are among the most complex and accident-prone elements of modern traffic networks, accounting for 43% of the total injury causing accidents and 21% of the vehicle related fatalities in Europe [1]. Moreover, recent numbers indicate that a majority of the accidents at intersections are caused by drivers' errors [2], often as a result of misinterpretation of a situation, inattention or the disregard of traffic rules. Therefore, new Advanced Driver Assistance Systems (ADAS) have to cope with highly complex traffic scenarios, as urban intersections with many lanes, where the behavior of the different road users is hardly predictable. In such scenarios, sensing the surrounding environment and assessing possible threats are challenging problems. Several recent works focused on these problems. In [3], an approach for situation analysis is provided, based on motion predictions and using object-oriented Bayesian networks to infer the probability of collision with all surrounding vehicles, and where traffic rules, the digital street map and the sensors' uncertainties are also considered. A map-based long term motion prediction is also proposed in [4], based on a stochastic filter able to determine the set of reasonable future trajectories for all detected vehicles in the current traffic situation. In this algorithm, where additional information from a digital map is used, the traffic lanes are represented by their corresponding centerlines where each detected vehicle is projected. Unlike most approaches in the literature, [5] presents a solution not based on trajectory prediction. Instead, dangerous situations are identified by comparing what drivers intend to do with what they are expected to do.

In this work, we will focus our attention on frontal collision scenarios, as depicted in Fig. 1. The underlying estimation/control problem is therefore divided in three main parts: motion prediction, threat assessment, and vehicle control. There are a number of interesting works on motion prediction available on the literature. Among many others, a predicting method for vehicle movements using Monte Carlo sampling is provided in [6]. Similarly, [7] uses Markov Chains to derive a probabilistic danger map of moving obstacles. More recently, [4] uses an Extended Kalman Filter together with digital map information for path predictions. On the other hand, collision detection and threat assessment algorithms assuming vehicle-to-vehicle communication have been studied in [3], [8], [9] and a polygon-based approach proposed in [9], [10] for identifying a potential threat and the collision interval. However, none of the aforementioned papers defines or provides a formal method in a probabilistic setting. Finally, several control approaches tried to incorporate the so called "point of no return", i.e., configurations from which a collision cannot be avoided. Two interesting algorithms are presented in [11] and [12], for example. Other works have approached this same problem using reachability analysis [13]. For instance, [14], [15] focus on autonomous negotiation algorithms for traffic intersections.

This paper proposes an active-safety system for frontal collisions detection and prevention/mitigation targeting the following objectives: (i) Design of a probabilistic path prediction of the surrounding vehicles; (ii) Develop an efficient probabilistic collision detection algorithm; (iii) Assess, in a formal and robust way, the necessity of an intervention; (iv) Overtake the driver if considered necessary. Considering the previous

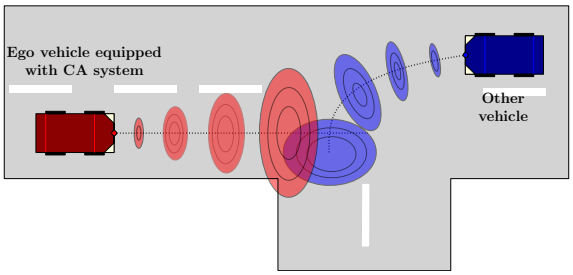

Fig. 1. Illustration of the proposed probabilistic approach. In this image, the ego vehicle corresponds to the red car, while the other vehicle is presented in blue. Furthermore, the probability densities (blue and red clouds) concern the vehicles' front bumpers at different time steps.

* This work is supported by ÅF, DENSO, Chalmers' Area of Advance in Transportation, SAFER and the Department of Signals and Systems (S2).

[1] Department of Signals and Systems (S2), Chalmers University of Technology, Göteborg, Sweden.
Email: gabriel.campos,paolo.falcone@chalmers.se
[2] ÅF, Göteborg, Sweden.
Email:adam.fjeldsted,fredrik.granum@afconsult.com
[3] DENSO International Europe, Göteborg, Sweden.
Email: k.alenljung@denso.se

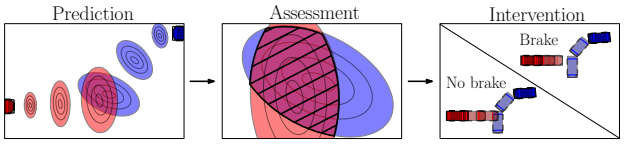

Fig. 2. An illustration of the different problems tackled by the proposed solution: **P1**.- predict the positions of the oncoming traffic ; **P2**.- assess a collision threat; **P3**.- trigger an intervention at an appropriate moment.

problems, the contributions of this work are threefold: (i) a probabilistic motion prediction algorithm based on an Unscented Kalman filter (UKF); (ii) a formal calculation method of the collision probability based on a Euclidean vector space defined by reference points on the vehicles' structure; (iii) a reachability-based decision-making protocol regarding the necessity of an intervention.

II. Problem Description

Consider the scenario depicted in Fig. 1. For the sake of the scenario simplicity, we assume that the ego (red) vehicle is not turning. Note that the vehicles travelling on the opposite direction will be called throughout the rest of the article as the "other vehicle", and the corresponding variables denoted with the superscript $\bar{(.)}$. The proposed solution is on-board sensor-based. Therefore, the considered scenarios assume that vehicles are in line of sight with respect to a given sensor such as, for example, a radar. Furthermore, we assume that the ego vehicle is equipped with the proposed Collision Avoidance (CA) system. There are three problems to be solved:

- **P1**. Predict the evolution of oncoming vehicles, given a dynamical model describing their motion;
- **P2**. Evaluate the probability of a collision;
- **P3**. Intervene, as late as possible, in order to avoid or mitigate a collision.

An illustration of the different problems to be tackled by the proposed safety strategy is presented in Fig. 2.

Remark 1: Though the motion of the ego vehicle is assumed here to follow a straight path, the extension to turning maneuvers simply requires an appropriate modeling of the other vehicle's motion with respect to a rotating reference frame.

III. Vehicle Model

In this work, we consider that the motion of both cars obeys to a traditional unicycle model with constant turn rate and acceleration (CTRA), i.e., assuming that a driver will most likely drive with a constant turn rate and acceleration [16]. Furthermore, the accelerations in the lateral and longitudinal directions are separately constrained as in [6]. We assume the origin of the coordinate frame to be the ego vehicle's sensor position (the middle point of the front bumper), and that predictions are made with respect to the front bumper of the different cars. We consider that the ego vehicle is equipped with inertial sensors that measure its own speed, acceleration and yaw rate. Moreover, the range R, the azimuth angle ϕ, and the speed, yaw angle and length of the other vehicle are also considered to be measured. An illustration of the sensing convention is provided in Fig. 3.

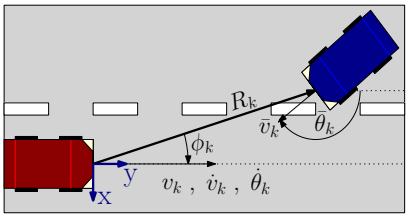

Fig. 3. Illustration of the considered scenario: the reference frame is positioned at the current position of the front bumper of the ego vehicle.

Let k denote the time step and let $(.)_k$ represent the value of a variable at time k. Let ω_1, ω_2 be two control parameters such that ω_1, $\omega_2 \in \{-1, 1\}$. More precisely, the two different values of ω_1 and ω_2 define if the vehicle is going forward or backwards or if the car is turning right or left, respectively. The considered dynamical vehicle model[1] is given as follows:

$$\dot{x} = v\sin(\theta), \tag{1a}$$

$$\dot{y} = v\cos(\theta), \tag{1b}$$

$$\dot{v} = \begin{cases} \omega_1 a_f, & \text{if } v \le v_{long}, \\ \omega_1 \frac{\kappa/v+\alpha_f}{2} + \frac{\kappa/v-\alpha_f}{2}, & \text{if } v > v_{long}, \end{cases} \tag{1c}$$

$$\dot{\theta} = \begin{cases} v\sin(\theta_{max}\omega_2)/l, & \text{if } v \le v_{lat}, \\ a_f\omega_2/v, & \text{if } v > v_{lat}, \end{cases} \tag{1d}$$

where (x, y) is the position, v the velocity and θ the heading angle. Furthermore, the maximum acceleration due to the road friction is denoted as a_f, θ_{max} is the maximum steering angle, l is the wheelbase and κ is a parameter describing the engine power. Moreover, v_{long} and v_{lat} are the breakpoint velocities at which the limit of the longitudinal acceleration switches from tyre-to-road friction to engine power and from maximum steering angle to tyre-to-road friction, respectively. Note that the velocity of the different vehicles is assumed to be bounded such that $0 \le v_k \le v_{max}$, where v_{max} is taken to be $50\ km/h$ for an urban area.

For the clearness of notation, define $\chi_k = \begin{bmatrix} x_k & y_k & v_k & \dot{v}_k & \theta_k & \dot{\theta}_k \end{bmatrix}^T$ as the ego vehicle's state vector, where $\dot{v}$ and $\dot{\theta}$ denote the acceleration and yaw rate, respectively. We can then establish:

$$\chi_{k+1} = f(\chi_k, u_k), \tag{2}$$

where f represents the unicycle model described in equation (1) and $u_k = \begin{bmatrix} \dot{v}_k & \theta_k \end{bmatrix}^T$ denotes the control input function given by the longitudinal acceleration and yaw rate, respectively. Furthermore, the measured states γ are defined as $\gamma_k = H\chi_k + W_k = H\chi_k + \begin{bmatrix} 0 & 0 & \sigma_v & \sigma_{\dot{v}} & \sigma_\theta & \sigma_{\dot{\theta}} \end{bmatrix}^T$, where H is the observation matrix and σ_v, $\sigma_{\dot{v}}$, σ_θ, $\sigma_{\dot{\theta}}$ denote the measurement noise on the speed, acceleration, yaw angle and yaw rate, respectively.

Define $\bar{\chi}$ as the state vector of the other vehicle, defined by augmenting χ with the position of the rear bumper. Thus, it follows:

$$\bar{\chi}_{k+1} = f(\bar{\chi}_k, \bar{u}_k), \tag{3}$$

where $\bar{\chi}_k$, $\bar{u}_k$ and $\bar{\gamma}_k = \bar{H}(\bar{\chi}_k)\bar{\chi}_k + \bar{W}_k$ are defined as for the ego vehicle. Note that $\bar{H}(\bar{\chi}_k)$ is a nonlinear equation.

[1]Accordingly to [6], a typical car is defined by the following parameters: $size = 1,8 \times 4,8\ m$, $l = 2,4\ m$, $a_f = 9,1\ m.s^{-2}$, $\kappa = 66,6\ m^2.s^{-3}$, $v_{lat} = 6,76\ m/s$, $v_{long} = 7,32\ m/s$ and $\theta_{max} = 0.5\ rad$. Note, however, that in this work we consider $a_f = 8.5\ m.s^{-2}$ as the maximum deceleration, a value obtained for our 2010's Volvo $S60$ T6 test vehicle.

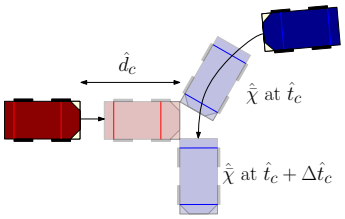

Fig. 4. A frontal collision scenario: illustration of the important parameters for collision avoidance systems, i.e., the predicted distance to collision $\hat{d}_c$, time to collision $\hat{t}_c$ and collision time interval $\hat{\Delta}t_c$.

IV. Motion Prediction

The path prediction algorithm proposed here is based on an Unscented Kalman Filter (UKF) subject to non-additive process noise. To the best of the authors knowledge, an UKF-based solution has not been considered so far in literature for this type of scenario. This choice is motivated by the need of accurately propagating the probability distributions throughout the safety system. Further details on a UKF and its advantages are provided in [17]–[19].

Regarding the ego vehicle (and identically for the other vehicle), the UKF consists of two alternating steps: (i) a-priori estimation using a motion model to generate the ego's (or the other vehicle's) states at future time steps; (ii) a-posteriori estimation filtering out the measurements noise in order to refine the states calculated at step (i).

- **A-priori estimation:** Consider the dynamical model (2). Denote the input by $\tilde{u}_k = u_k + \tilde{w}_k$ where $\tilde{w}_k \sim \mathbb{N}(0, Q_k)$ and the process noise is captured by the covariance matrix $Q_k = \begin{bmatrix}\sigma_{\hat{v}}^2 & 0; 0 & \sigma_{\hat{\theta}}^2\end{bmatrix}$. By performing an a-priori estimation based on function **f**, where **f** represents the unicycle model (2), the state estimate can then be expressed as $\hat{\chi}_k^-$ and the *a-priori* estimate covariance matrix denoted by P_k^-.
- **A-posteriori estimation:** The update step corrects the state prediction $\hat{\chi}_k^-$ by considering a new measurement, γ_k. In particular, given an observation equation H, we can obtain the predicted measured states $\hat{\gamma}_k$, the expected covariance of the measurements $\tilde{S}_k$ and the cross correlation C_k. Thus, the covariance matrix of the measurements, the Kalman gain, the updated state estimate and the a-posteriori estimated covariance matrix are given as, respectively, $S_k = \tilde{S}_k + R_k$, $K_k = C_k S_k^{-1}$, $\hat{x}_k = \hat{x}_k^- + K_k(\gamma_k - \hat{\gamma}_k)$ and $P_k = P_k^- - K_k S_k K_k^T$.

For the sake of brevity, the complete details will be omitted in this manuscript but they are available in [18], [20].

V. Collision Detection

Evaluating the risk of a collision when two conflicting paths merge is a key component of the proposed CA system. In this paper, we propose a new approach where a vectorial space (representing a collision) is defined and compute the probability of the estimated vectors (connecting the two vehicles) lying within the collision space. In the sequel, we characterize all the positions, with respect to the reference

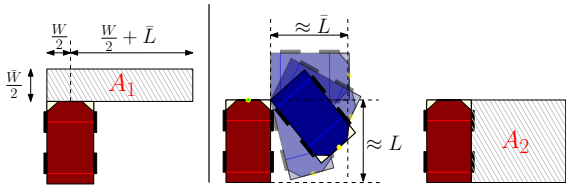

Fig. 5. Illustration of vectorial spaces A_1 and A_2 representing an effective collision.

frame placed at the ego vehicle's front bumper, that correspond to a collision[2].

With respect to the middle point of the front bumper of the ego car, it is possible to define two convex Euclidean spaces, denoted by A_1 and A_2. An illustration is provided in Fig. 5, where L and W denote the length and width of the ego vehicle, respectively, while $\bar{L}$ and $\bar{W}$ are the length and width of the other vehicle. Note that, although the length of the other vehicle is assumed to be known, it is possible without loss of generality to redefine new collision boxes based on real-time measurements of the other vehicle's length. Furthermore, and in order to capture the duration of a collision, the evolution of the rear bumper of the other car needs to be taken into consideration. Thus, a collision-free area, denoted by A_3, can be derived as depicted in Fig. 6. It is important to mention that A_3 differs by definition from A_2, since here the target point is the middle point of the rear bumper. Indeed, if the projection of the position of rear bumper of the other vehicle lies within A_3, then the collision risk is null at that time instant.

In order to design an efficient collision avoidance system, the probability of a collision still needs to be computed. In the sequel, we propose a solution based on vectors connecting the front bumper of the ego vehicle and the front and rear bumper of the other vehicle, which are represented by bivariate normally distributed variables. In order to derive the probability of a collision, the joint cumulative distribution can be computed by determining the probability distribution over the areas of interest such as:

$$P_{Collision} = \int\int_{A_1} P_1(x,y)\mathrm{d}x\mathrm{d}y + \int\int_{A_2} P_1(x,y)\mathrm{d}x\mathrm{d}y, \quad (4)$$

where the bounds of the integrals are defined by the upper and lower bounds of the collision zones A_1 and A_2 on the corresponding axis. In an identical way, it is possible to compute the probability of a collision-free evolution such as:

$$P_{Free} = \int\int_{A_3} P_2(x,y)\mathrm{d}x\mathrm{d}y, \quad (5)$$

knowing that P_1 and P_2 are bivariate normal distributions describing the vector between the front bumpers of the two vehicles and the vector between the ego's front bumper and other vehicle's rear bumper, respectively. Further details on the online computation methods of the joint cumulative distribution are provided in [21].

[2] Note that the proposed collision zones may lead to some conservativeness, since they may capture configurations that do not effectively lead to a frontal collision but to very close crossing-trajectories. However, if one considers that drivers may have a comfort zone, that is, a minimum distance separating vehicles in these type of maneuvers, it is our believe that the current collision definition may cope with comfort/safety parameters.

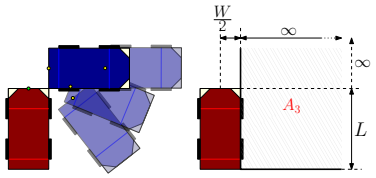

Fig. 6. Illustration of the collision-free area A_3 defined with respect to the rear bumper of the other vehicle.

Define d_c and t_c as the distance and time to collision, respectively. Furthermore, let Δt_c denote the time needed for the other vehicle to leave the collision area, see Fig. 4. By combining the predictions given by the UKF with equations (4) and (5), the probability of a collision can then be computed. Moreover, the estimates $\hat{t}_c$, $\hat{\Delta t}_c$ and $\hat{d}_c$ and the respective probability distributions can also be derived. It is worth mentioning that in order to guarantee a certainty level on the threat assessment, a user-defined threshold $\mathcal{C}_1$ will be considered. In other words, only $P_{Collision} > \mathcal{C}_1$ will be taken as a serious threat. Note that $\mathcal{C}_1$ should generally be set to a high value in order to avoid false interventions on non-threatening situations. For further details, the reader can refer to [20].

Remark 2: The prediction of $\hat{d}_c$ is strictly related to the predicted $\hat{t}_c$ such that when the latter is under or overestimated, $\hat{d}_c$ will increase/decrease accordingly. Indeed, $\hat{d}_c$ is computed by the distance possibly travelled during $\hat{t}_c$ seconds, based on the predicted speeds and accelerations. This yields that the uncertainty on $\hat{d}_c$ is not captured as an uncertainty on the collision point, but rather as the uncertainty on the computation of the distance the ego vehicle can travel over that time.

VI. Collision avoidance

In this section, we will present the main principles behind the proposed decision-making protocol and intervention algorithm. We are particularly interested in identifying the so called "point of no return", from which a collision is unavoidable. The contribution of this article relies on a formal decision-making protocol regarding the need of an immediate intervention. More precisely, reachability analysis tools have been used for the derivation of simple, yet formally verifiable safety conditions. It will be shown that the proposed algorithm guarantees safety, avoiding the collision area for the risky period while integrating the uncertainties connected to the estimation of the distance to collision $\hat{d}_c$. Furthermore, this approach aims to minimize the amount of false interventions by intervening as late as possible but always before the point of no return, assuming that the available time and information are sufficient. The following definition is taken from [13].

Definition 1 (One-step and z- step controllable sets): Consider a system subject to external inputs described by $\chi_{(k+1)} = f(\chi_k, u_k)$, where $\chi_k \in \mathcal{X}$, $u_k \in \mathcal{U}$, and $k \geq 0$. We denote the one-step controllable set to the set $\mathcal{T}$ as:

$$\mathrm{Pre}(\mathcal{T}) \triangleq \{\chi \in \mathcal{X} \ : \exists u \in \mathcal{U} \text{ s.t. } f(\chi, u) \in \mathcal{T}\}.$$

Furthermore, the z-step controllable set $\mathrm{K}^z(\mathcal{T})$ to the set $\mathcal{T}$ is defined recursively as follows, where $m \in \{1, \ldots, z\}$:

$$\mathrm{K}^m(\mathcal{T}) \triangleq \mathrm{Pre}(\mathrm{K}^{m-1}(\mathcal{T})) \cap \mathcal{X}, \quad \mathrm{K}^0(\mathcal{T}) = \mathcal{T}. \qquad \square$$

In other words, $\mathrm{Pre}(\mathcal{T})$ is the set of states which can be driven into the target set $\mathcal{T}$ in one time step whereas all states belonging to the z-step controllable set $\mathrm{K}^z(\mathcal{T})$ can be driven, by a suitable control sequence, to the target set $\mathcal{T}$ in z steps while satisfying input and state constraints.

The *critical set* $\mathcal{S}$ (target set), representing a collision between the two vehicles and parameterized with respect to the distance to collision, is defined as follows:

$$\mathcal{S}_k = \begin{Bmatrix} \hat{d}_c | & 0 & \leq & \hat{d}_c & \leq & d_{max} \\ \hat{v} | & 0 & \leq & \hat{v} & \leq & v_{max} \end{Bmatrix}, \tag{6}$$

where v_{max} is the maximum allowed speed and d_{max} represents the maximum distance traveled over the prediction horizon if the vehicle is traveling at v_{max}.

Consider Definition 1. In order to capture the individual degree of freedom of the ego vehicle with respect to a potential collision, we are interested in determining if there exists a trajectory leading the ego vehicle to the critical set in a finite number of steps, under any feasible control input. Thus, we introduce here the notion of *attraction set*, denoted by $\mathcal{A}_i$, which corresponds to i-step controllable set $\mathrm{K}^i(\mathcal{S})$. In other words, the set $\mathcal{A}_i$ includes all possible state configurations that will lead the ego vehicle, unavoidably, to its *critical set* $\mathcal{S}$ in i steps given a constrained acceleration such that $-\alpha_f \leq \dot{v}_k \leq 0$. The reader can refer to [13] for further details on reachability analysis.

Consider that predictions on the time to collision $\hat{t}_c$ and collision duration $\hat{\Delta t}_c$ are available from the estimation algorithm presented in Section V. It follows from the definition of the attraction sets that in order for a collision to be avoided during the interval $t \in [\hat{t}_c, \hat{t}_c + \hat{\Delta t}_c]$, the following condition needs to be satisfied:

$$\chi_k \notin \mathcal{A}_{\hat{t}_c + j}, \quad \forall j = 0, ..., \hat{\Delta t}_c. \tag{7}$$

For obvious reasons, it is not enough to verify (7) at each time step in order to guarantee a collision-free trajectory. Indeed, if (7) is not satisfied at the current instant, then a collision is already unavoidable and can only be mitigated. Furthermore, it is also important to incorporate the vehicles reaction time t_r, assumed to be equal to the time it takes for the vehicle to build up full brake pressure and also known as the ramp up time.

Given the current state and the predictions provided by the UKF-based prediction algorithm, the emergency braking procedure should be triggered if the following condition is satisfied:

$$\hat{\chi}_{t_r+1} \in \mathcal{A}_{(\hat{t}_c + j) - (t_r + 1)}, \quad \forall j = 0, ..., \hat{\Delta t}_c, \tag{8}$$

where $\hat{\chi}_{t_r+1}$ represents the state vector of the ego vehicle predicted $t_r + 1$ steps in the future. If (8) is true, then a collision will be unavoidable in $t_r + 1$ steps. Thus, an intervention should be triggered immediately in order to avoid it.

By taking advantage of the structure of the problem, formal safety expressions are given in (7) and (8), where safety can be guaranteed by performing set-memberships tests verifying these two conditions. Note that (8) incorporates both the vehicle's reaction time and predicted motion profile in order to access the latest moment to trigger an intervention. It is however important to also consider the process noise, since

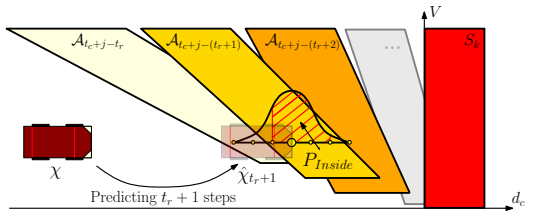

Fig. 7. Illustration of the proposed probabilistic decision-making procedure. Considering a normally distributed state prediction $\chi_{(t_r+1)}$, set-memberships tests accordingly to equation (8) are performed for several discrete points over the distribution.

such may critically influence certain parameters. Thus, it is crucial to develop an efficient decision-making protocol in a probabilistic setting. The main idea behind the proposed approach is depicted in Fig. 7 and explained as follows. Assuming that the uncertainty on $\hat{d}_c$ is normally distributed, it is then possible to compute the probability of the predicted state $\hat{\chi}_{t_r+1}$ belonging to a given attraction set, denoted by P_{Inside}, by performing set-membership tests for several discrete points over the distribution. By comparing such value with a user-defined threshold $\mathcal{C}_2$, defining the level of certainty of the decision-making algorithm, a choice regarding an intervention can be securely made. The reader can refer to [20] for a thorough explanation of the proposed algorithm.

VII. Results and Simulations

Consider an intersection scenario as illustrated in Fig. 1, where two cars travelling in opposite directions risk to be engaged in a frontal collision satisfying the initial assumptions. Considering the initial position/configuration of the ego vehicle, a collision will take place, in absence of a intervention, at $t_c = 9.04s$. However, given the other car's original/desired motion profile, the collision area would have been released by $t = 9.2s$. Therefore, this yields that there is a collision threat for a period of $\Delta t_c = 0.16s$. Recall that upon a detection of a collision, a braking intervention should be triggered, where the reaction time related to the brakes' pressure build-up is set to be $t_r = 0.24s \simeq 3\Delta t$ and $a_f = 8.5\ m/s^2$, accordingly to [22]. In this work, the time step of the system has been set to $\Delta t = t_{k+1} - t_k = 0.08s$, defining the update ratio of all the different system's components. Let also $\mathcal{C}_1 = 90\%$ and $\mathcal{C}_2 = 50\%$ be two tunable parameters controlling the sensitivity of the CA system: the first defines the confidence factor on the collision' probability computation; the second the confidence factor on the decision-making protocol. Regarding the process noise, the following process matrices are considered:

$$Q_p = \begin{bmatrix} 0.35^2 & 0 \\ 0 & 0.0135^2 \end{bmatrix} \Delta t^2,\ Q_e = \begin{bmatrix} 4 & 0 \\ 0 & 0.3 \end{bmatrix} \Delta t^2,\ Q_o = \begin{bmatrix} Q_e & 0 \\ 0 & Q_e \end{bmatrix},$$

where the Q_e and Q_o are used within the filtering algorithm for the ego and other vehicle, respectively, and Q_p for predictions. For the derivation of the following results, it is worth mentioning that realistic data has been used. This data was collected in two real vehicles equipped with highly accurate inertial measurements and GPS units, where the motion of the vehicles was subject to a longitudinal offset due to obvious safety reasons. The collected data, where the offset was eliminated, has later been used for different simulation setups considering realistic noise levels.

Fig. 8 illustrates the performance of the proposed system taking into consideration different noise levels on the measurements. Consider Fig. 8(a). One can see that a collision is detected at $t = 8.24s$ and the intervention triggered at $t = 8.40s$. Given the reaction time t_r, this yields that braking is initiated at $t = 8.64s$, very close to the optimal braking procedure [3], initiated at $t = 8.67s$. On the other hand, it follows from Fig. 8(b) that the predicted $\hat{t}_c$, illustrated by the dashed red lines, is in fact an accurate prediction. The duration of the collision, however, is slightly overestimated. Though, it is clear from the evolution of the full blue line that the collision is avoided and therefore safety is guaranteed. It also worth comparing this result with the theoretical one. By comparing the green and blue trajectories, it follows that the introduced conservativeness is related to the estimation error on $\hat{\Delta}t_c$. However, this results clearly show the potential and effectiveness of the proposed algorithm. Take now Fig. 8(c) and 8(d), where noisy measurements are considered. As expected, both the predicted $\hat{t}_c$ and $\hat{\Delta}t_c$ lack of accuracy, as one can see by comparing the expected collision interval (illustrated by the vertical black lines) and the real collision interval (dashed red lines). Same conclusion can be driven regarding the distance to collision prediction $\hat{d}_c$, also less accurate as it can be seen by the evolution of the blue crosses. Despite a later detection, however, an intervention has been triggered at an appropriate time and safety guaranteed, showing that the proposed system is robust to fairly high noise levels on the measurements.

VIII. Conclusions

This paper proposes a new, efficient probabilistic collision detection and decision-making algorithm for safety interventions at traffic intersection. More precisely, this algorithm has been designed for detecting and avoiding frontal collisions, a particularly challenging manoeuver. Firstly, we have proposed a probabilistic path prediction algorithm based on a unscented Kalman filter. Secondly, by defining the Euclidean space representing all possible conflicting configurations, an elegant threat assessment protocol has been proposed, able to detect with a certain degree of certainty a future collision. Finally, we have proposed a minimally invasive intervention protocol, based on a emergency braking triggered as late as possible. Several simulation and implementation results based on realistic data obtained for this specific scenario have shown the efficiency and potential of the proposed system. Furthermore, preliminary experimental results indicate that the proposed solution is real-time efficient and functional. Future works should include the knowledge of the road geometry/lane topology, different control principles other than emergency braking, as well as scenarios including more vehicles.

[3]The optimal behaviour is computed assuming perfect knowledge of the system. Given the true d_c, t_c and Δt_c, the latest possible moment for applying an emergency braking while still avoiding the collision is computed by backward iteration, with a very refined update ratio.

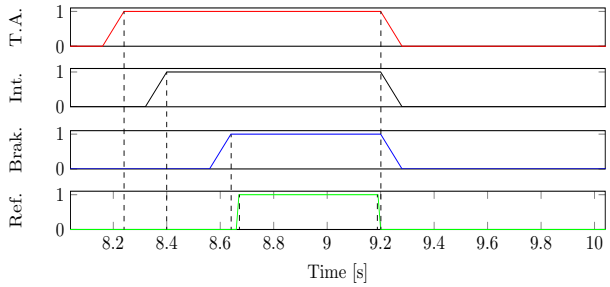

(a)

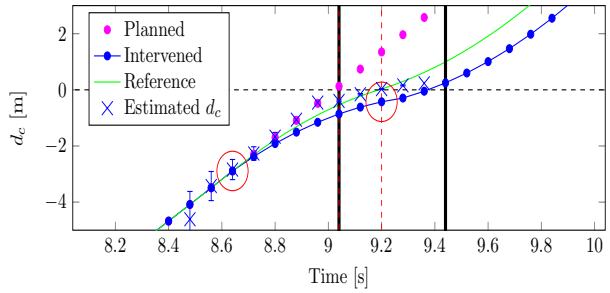

(b)

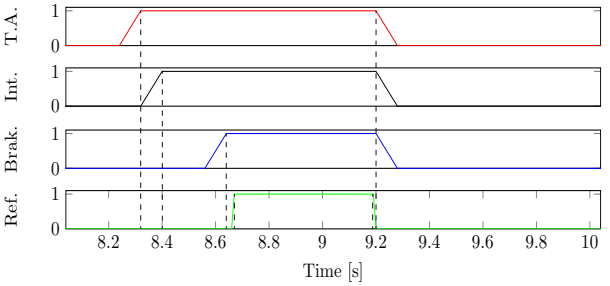

(c)

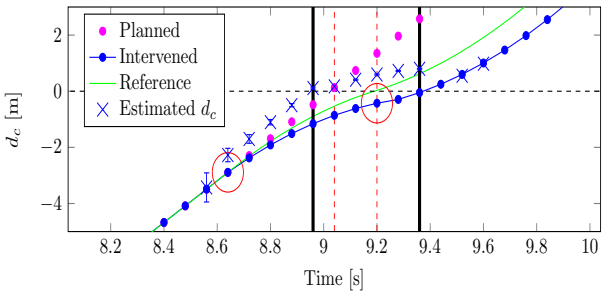

(d)

Fig. 8. An illustration of the active-safety system' behaviour: (a-b) without additional noise where $\sigma_v = 0.1\frac{m}{s}$, $\sigma_R = 0.01m$, $\sigma_\theta = 1\,^\circ$, $\sigma_\phi = 0.1\,^\circ$; (c-d) with additional noise where $\sigma_v = 0.5\frac{m}{s}$, $\sigma_R = 0.5m$, $\sigma_\theta = 2\,^\circ$, $\sigma_\phi = 1.375\,^\circ$. In figures (a),(c), from the top to the bottom, the first graph illustrates the time span where a threat has been identified by the threat assessment block; the second graph the time span during which a emergency braking has been triggered by the decision-making protocol; the third graph the brakes pressure-building procedure and the actual deceleration triggering instant; the bottom graph the *optimal* braking time assuming a perfect knowledge of the scenario. Moreover, the dashed lines highlight pertinent time instants. In figures (b),(d), the violet line represents the ego vehicle's initial/unaltered trajectory, the blue line the path resulting from the intervention of the CA system while the green line represents the desired/optimal behaviour of the collision avoidance system. Furthermore, the red dashed line represents the actual collision time interval, the solid black lines the estimated collision interval and the two red circles indicate when braking is initiated and stopped. Finally, the blue crosses illustrate the predicted (t_r steps in the future) mean of $\hat{d}_c$ and its variance illustrated by a blue vertical bar. Note that d_c is assumed to take negative values until collision.

REFERENCES

[1] M. Simon, T. Hermitte, and Y. Page, "Intersection road accident causation: A European view," *International Technical Conference on the Enhanced Safety of Vehicles*, 2009.

[2] A. Molinero Martinez, H. Evdorides, C. L. Naing, A. Kirk, J. Tecl, J. Barrios, M. Simon, V. Phan, and T. Hermitte, "Accident causation and pre-accidental driving situations. part 3: Summary report," 2008.

[3] G. Weidl, D. Petrich, D. Kasper, A. Wedel, G. Breuel, and S. Virat, "Collision Risk Prediction and Warning at Road Intersections Using an Object Oriented Bayesian Network," in *Conference on Automotive User Interfaces and Interactive Vehicular Applications*, 2013.

[4] D. Petrich, T. Dang, D. Kasper, G. Breuel, and C. Stiller, "Map-based long term motion prediction for vehicles in traffic environments," in *IEEE Conference on Intell. Transportation Systems*, 2013.

[5] S. Lefevre, C. Laugier, and J. Ibanez-Guzman, "Evaluating risk at road intersections by detecting conflicting intentions," in *IEEE/RSJ International Conference on Intell. Robots and Systems*, 2012.

[6] A. Eidehall and L. Petersson, "Statistical Threat Assessment for General Road Scenes Using Monte Carlo Sampling," *IEEE Transactions on Intell. Transportation Systems*, vol. 9, no. 1, pp. 137–147, 2008.

[7] F. Rohrmuller, M. Althoff, D. Wollherr, and M. Buss, "Probabilistic mapping of dynamic obstacles using markov chains for replanning in dynamic environments," in *IEEE/RSJ International Conference on Intell. Robots and Systems*, 2008.

[8] S. Kim, S. Lee, I. Yoon, M. Yoon, and D.-H. Kim, "The Vehicle Collision Warning System Based on GPS," *ACIS/JNU International Conference on Computers, Networks, Systems and Industrial Engineering*, 2011.

[9] Y. Wang, E. Wenjuan, D. Tian, G. Lu, G. Yu, and Y. Wang, "Vehicle collision warning system and collision detection algorithm based on vehicle infrastructure integration," in *Advanced Forum on Transportation of China*, 2011.

[10] M. Althoff, O. Stursberg, and M. Buss, "Model-Based Probabilistic Collision Detection in Autonomous Driving," *IEEE Transactions on Intell. Transportation Systems*, vol. 10, no. 2, pp. 299–310, 2009.

[11] M. Brannstrom, E. Coelingh, and J. Sjoberg, "Model-based threat assessment for avoiding arbitrary vehicle collisions," *IEEE Transactions on Intell. Transportation Systems,*, vol. 11, no. 3, pp. 658–669, 2010.

[12] N. Kaempchen, B. Schiele, and K. Dietmayer, "Situation Assessment of an Autonomous Emergency Brake for Arbitrary Vehicle-to-Vehicle Collision Scenarios," *IEEE Transactions on Intell. Transportation Systems*, vol. 10, no. 4, pp. 678–687, 2009.

[13] F. Borrelli, A. Bemporad, and M. Morari, "Predictive control," In preparation, 2014.

[14] G. R. Campos, P. Falcone, and J. Sjöberg, "Autonomous cooperative driving: a velocity-based negotiation approach for intersection crossing," in *IEEE Conference on Intell. Transportation Systems*, 2013.

[15] G. R. Campos, P. Falcone, H. Wymeersch, J. Sjöberg, and R. Hult, "A receding horizon control strategy for cooperative conflict resolution at traffic intersections," in *IEEE Conference on Decision and Control*, 2014.

[16] H. Godthelp, "Vehicle control during curve driving," *Human Factors*, vol. 28, no. 2, pp. 211–221, 1986.

[17] S. Särkkä, *Bayesian Filtering and Smoothing*. Cambridge University Press, 2013.

[18] S. J. Julier and J. K. Uhlmann, "A new extension of the kalman filter to nonlinear systems," in *Int. symp. aerospace/defense sensing, simul. and controls*, vol. 3, no. 26, 1997.

[19] M. Tsogas, A. Polychronopoulos, and A. Amditis, "Unscented Kalman filter design for curvilinear motion models suitable for automotive safety applications," *International Conference on Information Fusion*, 2005.

[20] A. H. Runarsson and F. Granum, *Path prediction and collision avoidance at intersections*. Master thesis, Chalmers University of Technology, 2014.

[21] Z. Drezner, "Computation of the Bivariate Normal Integral," *Mathematics of Computation*, vol. 32, no. 141, pp. 277–279, 1978.

[22] C. Grover, I. Knight, F. Okoro, I. Simmons, G. Couper, P. Massie, and B. Smith, "Automated emergency braking systems: Technical requirements, costs and benefits," Tech. Rep., 2008.